

RESEARCH ARTICLE

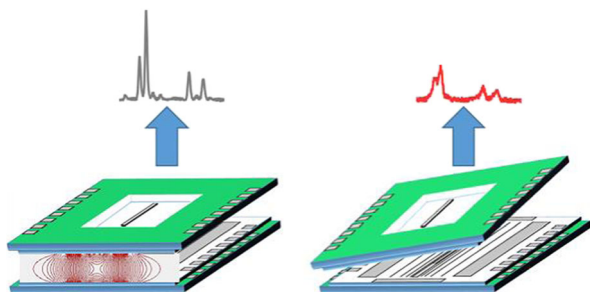
Experimental Observation of the Effects of Translational and Rotational Electrode Misalignment on a Planar Linear Ion Trap Mass Spectrometer

Yuan Tian,^{1,2} Trevor K. Decker,³ Joshua S. McClellan,³ Qinghao Wu,¹
Abraham De la Cruz,¹ Aaron R. Hawkins,³ Daniel E. Austin¹

¹Department of Chemistry and Biochemistry, Brigham Young University, Provo, UT 84602, USA

²Present Address: Department of Chemistry and Molecular Engineering, Zhengzhou University, Zhengzhou, 450001, Henan, People's Republic of China

³Department of Electrical and Computer Engineering, Brigham Young University, Provo, UT 84602, USA



Abstract. The performance of miniaturized ion trap mass analyzers is limited, in part, by the accuracy with which electrodes can be fabricated and positioned relative to each other. Alignment of plates in a two-plate planar LIT is ideal to characterize misalignment effects, as it represents the simplest possible case, having only six degrees of freedom (DOF) (three translational and three rotational). High-precision motorized actuators were used to vary the alignment between the two ion trap plates

in five DOFs— x , y , z , pitch, and yaw. A comparison between the experiment and previous simulations shows reasonable agreement. Pitch, or the degree to which the plates are parallel along the axial direction, has the largest and sharpest impact to resolving power, with resolving power dropping noticeably with pitch misalignment of a fraction of a degree. Lateral displacement (x) and yaw (rotation of one plate, but plates remain parallel) both have a strong impact on ion ejection efficiency, but little effect on resolving power. The effects of plate spacing (y -displacement) on both resolving power and ion ejection efficiency are attributable to higher-order terms in the trapping field. Varying the DC (axial) trapping potential can elucidate the effects where more misalignments in more than one DOF affect performance. Implications of these results for miniaturized ion traps are discussed.

Keywords: Linear ion trap (LIT), Geometry deviation, Displacement, Misalignment, Degrees of freedom, Mass resolution

Received: 27 January 2018/Revised: 8 March 2018/Accepted: 10 March 2018/Published Online: 5 April 2018

Introduction

Mass spectrometers (MS) are among the most widely used instruments for identifying unknown compounds or analyzing samples at trace amounts; the method is both informative and sensitive. In contrast to routine use of MS in the laboratory setting, portable MS is able to broaden applications and benefit areas in which samples are less conveniently brought into the lab [1–3]. To be portable, a MS requires some combination of smaller physical dimensions or weight and

lower power consumption. Efforts have been made to miniaturize several different types of mass analyzers including time-of-flight (TOF) [4–8], magnetic sector [9], quadrupole mass filter [10–12], and ion trap [13–17]. Ion traps in particular are a promising choice for making a portable MS. Traps have a smaller size compared with magnetic sector instruments [18] and are able to operate at a higher pressure (10^{-3} Torr) compared with TOF and most other analyzers [18]. Several efforts to miniaturize ion traps have produced devices that are lighter and lower power than their full-sized counterparts [19–24]. Approaches to miniaturize ion traps include simple size reduction, novel trap or electrode geometries, novel fabrication and construction techniques, and parallel arrays [20, 25–30].

Several issues arise when making highly miniaturized ion traps. For instance, the smaller trapping volume leads to increased space charge effects, in turn leading to reduced trapping capacity and sensitivity [31]. Surface roughness of electrodes can affect the accuracy of the trapping electric field [32]. The closer physical proximity of electrodes increases the potential for electric discharge [33] and increases electrical capacitance, both of which limit the magnitude of the applied trapping voltage [34]. The reduction in the trapping capacity due to space charge could be restored by the use of paralleling trap arrays [35–38] or, alternatively, by using a trap geometry with an extended trapping dimension, such as a linear ion trap (LIT) [13, 15, 39] or toroidal ion trap [17, 40, 41]. The absolute mechanical tolerances are generally improved by using microfabrication techniques [35–38, 42–44], but relative tolerances and alignment can become problematic at the small scale. Further, even if electrodes can be fabricated very precisely, there remains the potential for misalignment of electrodes as the trap is assembled. Whether in arrays or in high-volume traps such as the LIT, high performance requires that one or more critical dimensions be maintained over a distance much larger than the characteristic trapping dimension. This is the essence of the trade-off between sensitivity and selectivity in miniaturized mass analyzers. As sensitivity is recovered using an array or an extended trapping dimension, variations in critical dimensions degrade both resolution and mass accuracy and, hence, analytical selectivity.

3-D traps, including quadrupole and cylindrical ion traps, generally have higher tolerance to physical misalignment compared with 2-D traps; however, these typically also have a reduced trapping capacity. Schwartz et al. [13] demonstrated the sensitivity of electrode alignment in one dimension on performance in the original LIT. In that work, a 0.125-mm shim was inserted on one end of one X rod to create a “deliberate linear variation of r_0 with axial position.” Similarly, a shim was added under one corner of a rod to produce a “twist” misalignment, and the effects of both misalignments on peak width were presented. If the distance between the opposite two electrodes varies along the length of the trap, the electric field also varies, resulting in ions with the same mass-to-charge ratio being selectively ejected at different time points in a scan. Methods to improve electrode alignment precision in quadrupole mass filters (QMF) have also been explored [45, 46]. Electrode alignment in toroidal ion traps poses a similar challenge. To maintain a constant cross section at every point around the ring, the inner ring electrode, the outer ring electrode, as well as the top and bottom end plates should be perfectly aligned in three dimensions. For all these types of ion traps, due to the number of independent electrodes, the number of degrees of freedom (DOF) is quite high, making evaluation and control of alignment a difficult experimental problem.

Our group has shown that ion trap mass analyzers can be made using two plates, the facing surfaces of which are lithographically patterned with electrodes [47–50]. Trapping fields are created in the space between the two plates. Each plate is

lithographically patterned with very small dimensional tolerances (substrate planarity on the order of tens of nanometers and electrode positioning on the order of a micrometer). The accuracy of the electric fields in such a trap is limited primarily by the alignment of one plate with respect to the other. For example, in one experiment, the plates of a linear-type trap were aligned by four precision sapphire balls positioned into laser-drilled holes in each plate. When the same plates were brought closer from 4.38 to 1.9 mm using different sizes of sapphire balls, the performance varied significantly each time the plates were reassembled even in the same orientation [51]. In contrast, the two-plate planar Paul trap (3-D trap) similarly mounted did not show this behavior.

Calculations of the effects of electrode misalignment on a LIT were reported showing that a LIT made of rectangular electrode is more sensitive to translational deviation while a circular shape is more sensitive to angular deviation [52]. However, no experimental results of electrode misalignment have been presented since Schwartz’s work [13]. In the present paper, the effects of electrode alignment were experimentally demonstrated using a recent version of a two-plate planar LIT [53]. Alignment between the two plates involved only six degrees of freedom, far fewer than in ion traps made using machined or individually fabricated electrodes—the conventional LIT and RIT have 12 and 6 independent electrodes, respectively. The patterned plates (borosilicate glass substrates) were installed on a new assembly which has a series of motorized stages that can adjust four DOFs of one plate and another DOF on the other plate. The experimental performance, in terms of mass resolution and peak intensity, is presented and compared with prior simulation results. As the effects of electrode misalignment are common to many types of ion traps, miniaturized or otherwise, these results are broadly applicable.

Experimental

With one plate fixed, positioning of the other plate involves only six DOFs, as shown in Fig. 1. Individual modes of alignment are presented in Table 1, together with hypothesized symptoms of misalignment in each direction. Of course, in any real device, all six misalignments will be present simultaneously to some degree, and the expected effects may combine.

The pitch and yaw of the top plate relative to the fixed bottom plate are the most critical to good performance. Under these two types of misalignment, ions in different regions of the trap see different electric fields. Displacement in the x-direction and roll affect all ions equally and may lead to reduced ion ejection. Displacement in the y-direction is equivalent to the “electrode stretching” that is commonly done to optimize many other types of ion traps. This displacement changes the higher-order terms in the trapping field (octopole, dodecapole, etc.) and will also affect resonant excitation and ejection. Finally, displacement in the z-direction has minimal effect on ions near the center of the device, with stronger effects toward the ends.

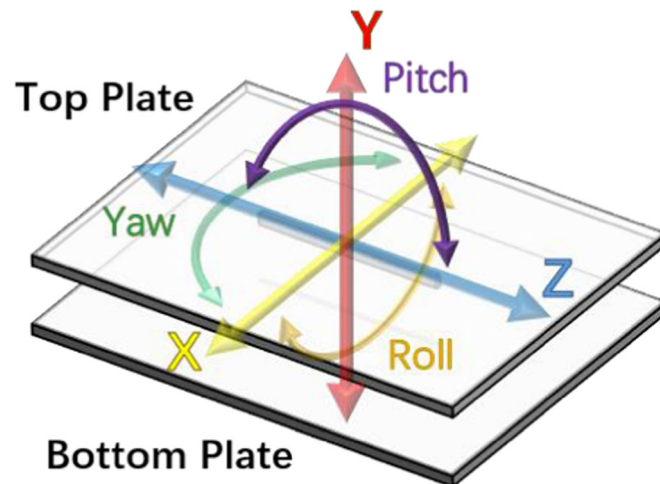


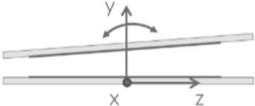
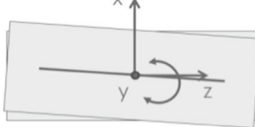
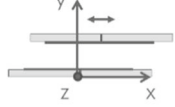
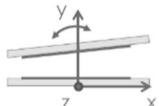
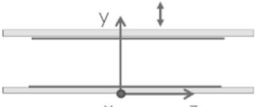
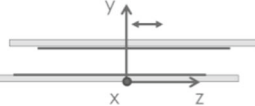
Figure 1. If the bottom plate is considered to be fixed, the top plate has six degrees of freedom of motion—three translational (x, y, and z) and three rotational (pitch, roll, and yaw)

Ion Trap Plates and Mounting

Plate fabrication is as reported previously [53]. In summary, 34 × 60-mm borosilicate glass substrates, 0.5-mm thick, were

machined with a tapered, 500- μm wide slit in the longitudinal direction. The trapping faces of the plates were lithographically patterned with a series of aluminum lines as electrodes that

Table 1. Misalignments Corresponding to Each of the Six Degrees of Freedom Between Two Patterned Plates, Together with Hypothesized Effects on Ion Trap Performance

Degrees of freedom	Types of misalignment	Importance to performance	Effects of misalignment
	Pitch	High	Measured mass varies along length of trap, resulting in reduced mass resolution
	Yaw	High	Ejection efficiency varies along length of trap, optimal at one point, possible effect on resolution as well
	X-displacement	Intermediate	Ion motion will couple in non-ejection direction, leading to reduced signal intensity
	Roll	Low	Possible ion losses during ejection
	Y-displacement	Intermediate	Changes higher-order terms of trapping field; mass resolution falls off above and below optimal spacing
	Z-displacement	Low	Possible effect on ions towards the ends; minimal effect in center

were wire bonded to printed circuit boards (PCB). The voltage applied on each electrode line was independently adjusted to form a quadrupolar electric field and compensate for any higher order components. Another set of PCBs with capacitors and spring-loaded pins was attached on the back side of the wire-bonded PCB so that voltages could be passed to the patterned glass plate.

Although it is possible to use a single, six-axis micropositioner for these studies, such a positioner was not available for this study. We instead opted to combine a motorized x,y,z stage with a rotational stage for one plate, and a previously built tile stage for the other plate, creating an alignment platform that allowed independently adjusting X-, Y-, and Z-displacements; yaw; and pitch (Fig. 2). Plate holders were used to fix the ion trap plates and PCBs together as well as to mount the assembly on the platform (Fig. 3). The top plate is mobile in the pitch direction. A one-dimensional motorized actuator (Z812V, Thorlabs, Inc.) was placed on the transverse side of the plate holder to adjust and control pitch. A spring was embedded on the opposite side to counterbalance the movement of the actuator and to reduce hysteresis of motion. A motorized xyz-stage (MAX343, Thorlabs Inc.) was also positioned on the base piece, and a motorized rotational stage (CR1-Z7K Thorlabs, Inc.) was centered on top of the XYZ stage. A channel electron multiplier (Detech, Inc.) was mounted between the platform and the bottom plate, surrounded by a copper shield. An electron gun (Torion Inc, American Fork, UT) was mounted on one of the side support to inject electrons into the trap in the longitudinal direction. The one-dimensional actuator controlling pitch has a travel range of 6 mm with a minimum step size of 50 nm; the bidirectional repeatability is less than 1.5 μm . The

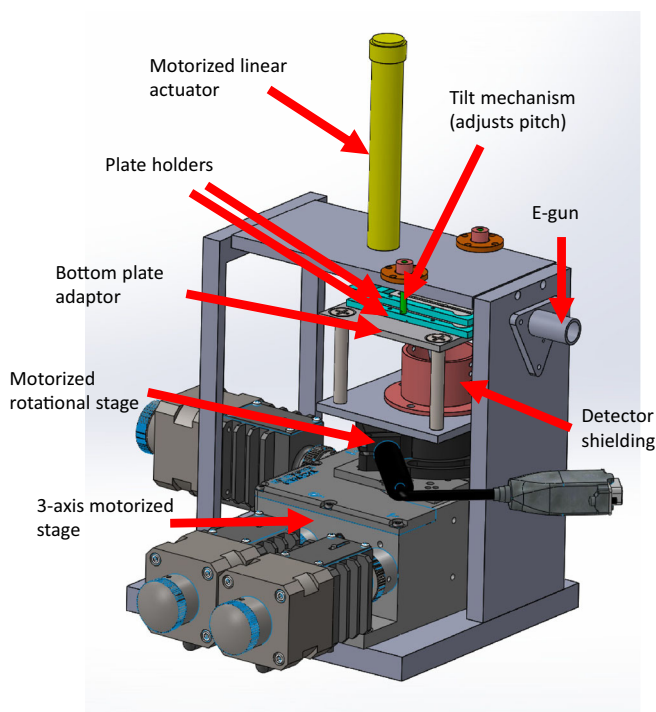


Figure 2. The 3-D assembly in SolidWorks

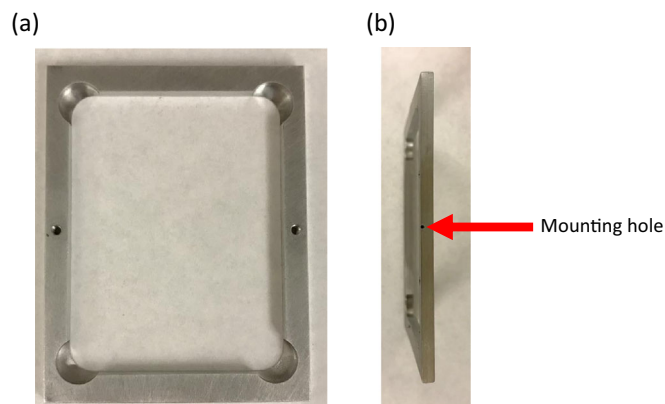


Figure 3. (a) Top view of the plate holder. (b) Side view of the plate holder

three-dimensional stage was installed with stepper motors that have travel ranges of 4 mm with 5 nm resolution and a bidirectional repeatability of 50 nm. The rotational stage has a repeatability of better than 1 arcminute.

With the previous setup, it is not possible to know in advance which settings on the micropositioners correspond to perfect plate alignment. However, precision sapphire balls were used to “pre-position” the plates into the assembly to provide a rough estimate of the positioner settings that correspond to optimal plate alignment. After mounting the plates, the bottom plate was retracted and these balls were removed. The bottom plate was returned to the original position prior to beginning experiments. In the following experiments, a single DOF was adjusted while all other DOFs were kept at the ball-aligned positions.

Experimental Conditions

A single-phase, 1.35-MHz radio frequency (RF) driving voltage of $200 V_{0-p}$ was provided by an Ardara RF power supply (Ardara, PA) and applied to the capacitive voltage divider. In addition, an AC waveform at a frequency of 620 kHz was applied to the top plate; the AC amplitude was $1 V_{0-p}$. The samples used included a mixture of toluene and deuterated toluene (D8) at a volume ratio of 1:1, and a mixture of xylenes. Samples were loaded in a 1-mL glass tube which was mounted onto a leak valve (203 variable leak, Granville Phillips, Boulder, Colorado). By slowly turning on the leak valve, the sample vapor was brought into the vacuum and the pressure raised from below 10^{-7} to $4-5 \times 10^{-6}$ Torr. After the sample pressure stabilized, another leak valve was opened to introduce helium, bringing the pressure to 3.6×10^{-3} Torr. The e-gun acceleration voltage was set to -62 V, and a waveform of -100 V/+23 V DC volts was applied to the e-gun gate to block or focus the electron beam. During the experiment, the RF voltage was ramped from 200 to 560 V_{0-p} over a period of 40 ms. The AC waveform, used for resonant ejection of ions, was only applied during the ramp. Each spectrum was averaged 20 times to improve the S/N ratio. Signals were amplified using a Keithley current amplifier (427) and recorded on an oscilloscope (WaveSurfer 42Xs, LeCroy).

Mass resolution and peak intensity in ion traps are affected by both the sample pressure and by the pressure of the buffer gas [54]. To reduce the effect of these variables, all experiments were conducted in sequence without breaking vacuum. The sample and buffer gas pressures were stable and were not adjusted during the sequence of experiments. The use of motorized actuators allowed plate adjustment in vacuum with high precision.

Results and Discussion

The angular deviation in pitch, as expected, has a large impact on both the resolution and the intensity. Figure 4a shows the spectra at different pitch angles for the toluene mixture. The reported pitch angles are based on the rough estimate of 0° as determined by the alignment balls (described previously). Thus, there may be an offset in the reported angles. Presumably, the best performance should correspond to optimal plate alignment, and in the absence of any mechanical hysteresis or any misalignment in the other DOFs, any effect should be symmetric with respect to positive and negative pitch angles. The “+” symbol represents the movement of stretching in the one-dimensional actuator, and the “-” symbol represents

retraction. In this design, the actuator stood on the opposite side of where the electron beam entered, so that the electron beam might be partially blocked if the negative pitch is too severe. The actuator’s travel range is 0.4 mm, corresponding to a variation from -0.32 to $+0.32^\circ$ in pitch. The position was varied 0.08° between scans.

A clear variation in the resolution can be seen as pitch angle changes. The m/z 91 and 92 peaks were completely separated at 0° and $+0.08^\circ$. Peak intensities were also the strongest in the range between these two positions, but the performance decreased when the top plate was further deviated. The m/z 91 and 92 peaks started to overlap when the pitch angle was larger than $+0.16^\circ$ or was smaller than -0.08° . Although m/z 98 and 100 from D8-toluene were always separated, peak widths were broadened at large pitch angles and the intensity varied so much that they almost disappeared at $\pm 0.32^\circ$. Similar results were observed in the spectra of the xylene mixture (not shown) at the angles 0 and $+0.08^\circ$ gave the best performance. At these angles, the peaks at m/z 105 and 107 were separated from the molecular ion peak m/z 106, though they overlapped at large pitch angles. There is a very small but measurable shift in the apparent mass of each peak, amounting to approximately 0.5 m/z unit over the range of pitch angles.

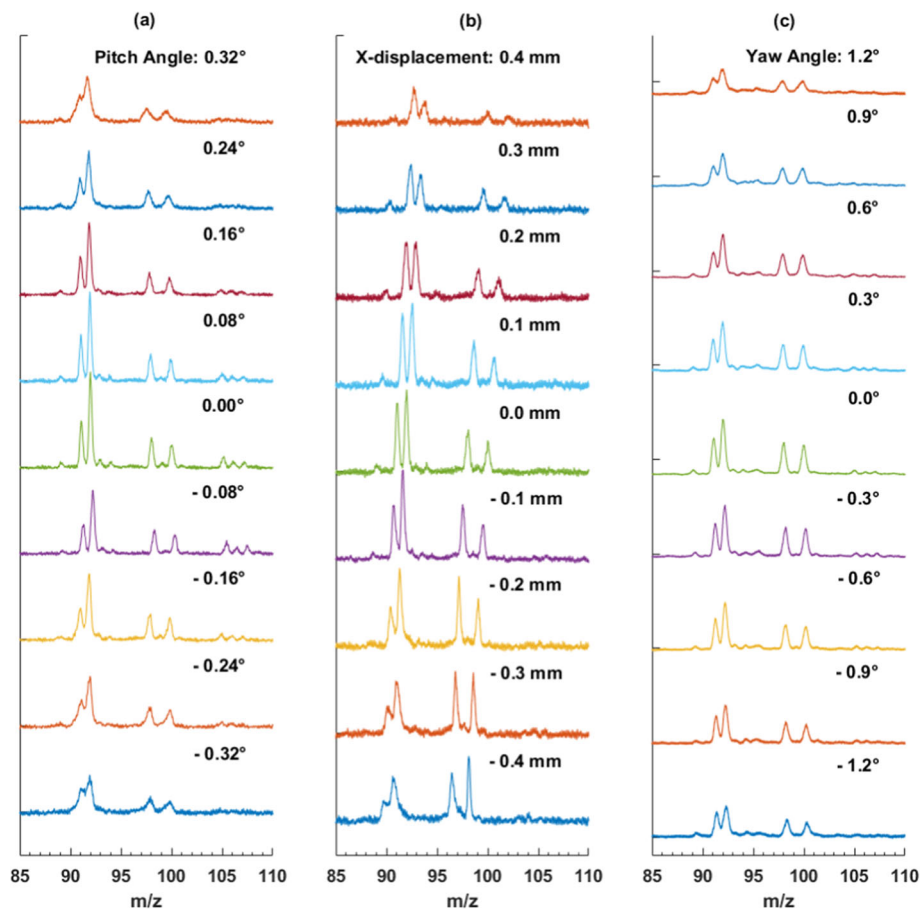


Figure 4. (a) The spectra at different pitch angles from -0.32 to $+0.32^\circ$. (b) The spectra with x-displacements deviated by different distances on two sides from -0.4 to $+0.4$ mm. (c) The spectra at different yaw angles from -1.2 to $+1.2^\circ$. All the spectra were calibrated based on the spectrum obtained at the assigned “zero” point

X-displacement, as predicted, should have less impact on the performance for small deviations. Figure 4b shows the spectra for the toluene mixture. Pitch angle was held at the 0° position. Again the “0 mm” x-position was an arbitrary point defined by the sapphire balls. Theoretically, there should be no difference between positive and negative displacement in x; however, the results were somewhat different between the two directions. The peak areas decreased over the range from +0.4 to -0.4 mm, but the 91 and 92 peaks became relatively stronger due to a higher resolution at around 0.00 mm position. The variation in peak areas followed what were predicted in the simulation—it generally decreased when x-displacement became larger—although with an offset. The differences between positive and negative x-displacement may be due to a physical asymmetry in the plates themselves, but could also be the result of residual misalignment in one or more of the other degrees of freedom. The data also showed a significant shift in the apparent mass as the plate alignment in the x-direction was varied. Over the range from 0.4 to -0.4 mm in x, peaks steadily shifted to lower mass by approximately 3 m/z units. The reason for this shift, and the reason for the asymmetry with respect to the assignment of zero, is unclear, although the asymmetry in peak areas was consistent with the shift in apparent mass.

Displacement in z was varied from -2.5 to +1.5 mm. Displacement from the z-direction, as expected, has little effect on the resolution (spectra not shown).

Mass spectra varied as the yaw angle was adjusted from -1.2 to +1.2° (Fig. 4c). Both resolution and ejection efficiency are affected by this variable. The addition of the yaw rotational stage took place after data were recorded for the other degrees of freedom, so any asymmetries in yaw data may not correlate with those in the other degrees of freedom. Variation in signal with yaw misalignment is likely due to the changing overlap of the electric potentials created by the two plates. For points where the slits are not aligned, the trapping field contains oblique terms that may hinder ion ejection through the slit.

Y-displacement, the equivalent of stretching the electrodes in conventional ion traps, was reported previously for this planar linear ion trap [53]. Misalignment in the roll direction is not expected to have a significant impact on trap performance and was not studied.

Figure 5 compares the previous experimental results and previously reported SIMION simulations [55] of the same effects. Figure 5 also includes previously published results [53] of changing the plate spacing (y-displacement) with the same plates. Each experimental data point is the average of three trials, and error bars represent standard deviations among these three trials. The position of each DOF was tested in both negative and positive positions in the experiment, whereas only positive positions were simulated—no asymmetry was expected in simulations.

The left column in Fig. 5 shows the variation of the width of the $m/z = 98$ peak under each misalignment DOF, for both experiment and simulation. It can be seen that the pitch appears to affect the resolution the most. Both the experiment and the simulation showed an abrupt change in the peak width within a

range of only 0.4° in pitch. Z-displacement seemed affect the resolution the least. X-displacement and plate spacing have similar impact on the resolution in the experiment, whereas simulation predicts the same impact from plate spacing but predict little impact from X-displacement. The degradation of the resolution caused by yaw deviations of 1° was at the same level as when pitch was deviated by 0.4° . Interestingly, the degraded resolution with yaw rotation seemed to be much stronger only in one direction, but not the other. It could be that the initial plate alignment was far enough off that the full range of yaw tests was all displaced in the same direction, or there could be other effects taking place.

The second column shows the peak area (as a surrogate for ion ejection efficiency) for different alignment positions, again comparing experiment and simulation. For unknown reasons, the peak intensity showed large variations during the pitch experiment, and no trend was evident. The variation of the peak area with x-displacement showed qualitative agreement between experiment and simulation, although with an offset that may be due to the assignment of “zero” in this direction or the combination with residual misalignment in other DOFs.

Peak area varies strongly with plate spacing, likely due to the effects on ion ejection efficiency due to higher-order terms in the trapping field. The plate spacing corresponding to the maximum peak area coincided with the spacing with the highest resolution—this is not required by symmetry nor is it an indication that the plates were aligned. Rather, this indicates that the electric field and/or ejection conditions that were optimal for rapid ejection were also optimal for efficient ejection of ions. Simulation and experimental results each showed a maximum peak area, but the falloff in simulations was much more gradual than that in the experiment. In both simulations and experiment, this falloff was asymmetric with respect to the optimal plate spacing. This asymmetry is not unexpected due to the higher-order terms of the trapping field. Differences between simulation and experiment point to factors that were inaccurately modeled in the simulations. A number of factors may be at play, including misalignment in other DOFs, subtle effects in the electric fields, and inaccuracies in device fabrication or in the capacitive voltage divider.

In the case of z-displacement, the peak intensity fluctuated in the experiment, and no trend was evident. On the other hand, the impact from yaw appears to be significant. The signal intensity dropped dramatically within $\pm 1^\circ$ of the optimal position. The fact that this feature is centered on 0° indicates that any offset between measured angle and actual angle was smaller than this value.

There was likely some residual misalignment in each of the DOF not being varied in a given experiment. The rough assignment of zero for each DOF seems to have been close, but the additive effect of all DOFs is difficult to predict. For instance, with a combination of x-displacement and yaw, the two ejection slits will line up perfectly at only one point, and this point will lie somewhere along the length of the trapping region, but not at the center where the highest ion density exists. The location of this point will shift as the x-

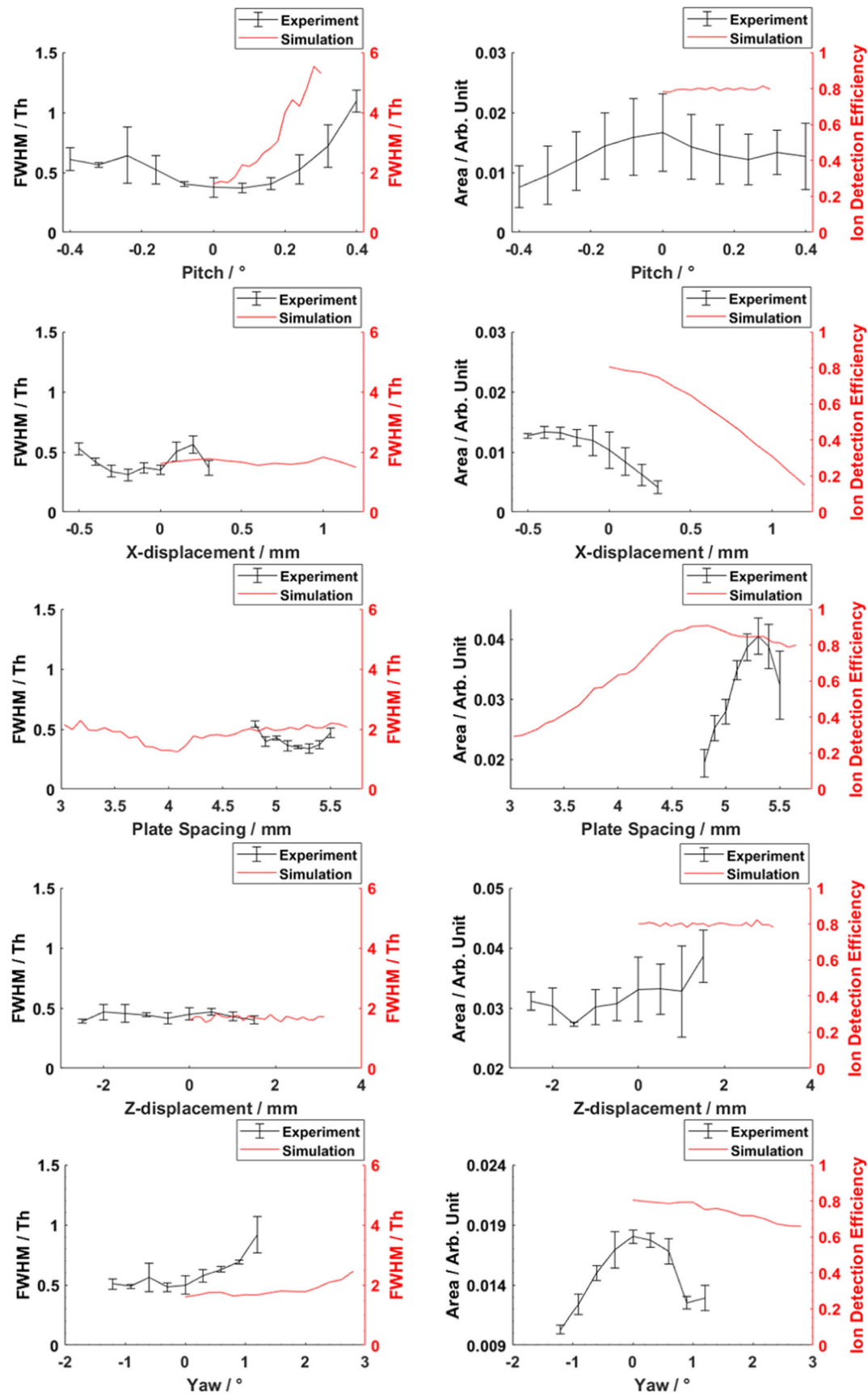


Figure 5. Comparison between experimental results and simulation results for variations in each degree of freedom studied

displacement is varied, although the zero point of the x-displacement or yaw is away from the actual zero position.

Schwartz et al. [13] demonstrated previously that changing the DC voltage applied to the ends of a LIT control how tightly the trapped ions are localized axially in the center of the trap. To explore whether a similar procedure would help assess pitch alignment in our experiment, a comparison between two pitch positions was compared. First, the top plate was placed at -0.24° . The DC voltage on the endbars was increased from 5 to 20 V. All the other DOFs were set to zero which were assumed to be the perfectly aligned positions. As seen in Fig. 6a, the resolution was largely unchanged with a higher applied DC. However, the signal intensity dropped off at higher values of the DC. This could be the result of more severe space charge, as ions were more tightly constrained, or may be due to the contribution of residual misalignment in other degrees of freedom. For comparison, the pitch angle of the top plate was then set to 0° and the experiment was repeated. The results were very similar between these two positions, so the ambiguity was not resolved.

However, from the data in Fig. 4, we saw that the zero-assignment in the x-direction may have had a significant offset—possibly by a few tenths of a millimeter. The DC potential applied to the endbars was varied for two positions of the x-displacement, -0.50 and $+0.50$ mm. As seen in Fig. 6c, d, the performance was entirely different on the two sides. An increase in DC voltage improved both the resolution and the peak intensity at -0.50 mm, whereas an increased DC voltage degrade both the resolution and the peak intensity at $+0.50$ mm. Likely, the -0.50 mm position had the cross-point closer to the middle of both plates. The $+0.50$ mm position had a cross-point farther away from that ideal position. Thus, a residual yaw displacement may have caused the asymmetry in the x-displacement results shown in Fig. 4c and Fig. 6c, d.

In practice, misalignments will usually involve contributions from each degree of freedom. However, the impact of each DOF may be independent. In the case of a conventional linear ion trap or toroidal ion trap made using metal electrodes, there are six DOFs between each combination of two electrodes. The cumulative effects of all possible misalignments

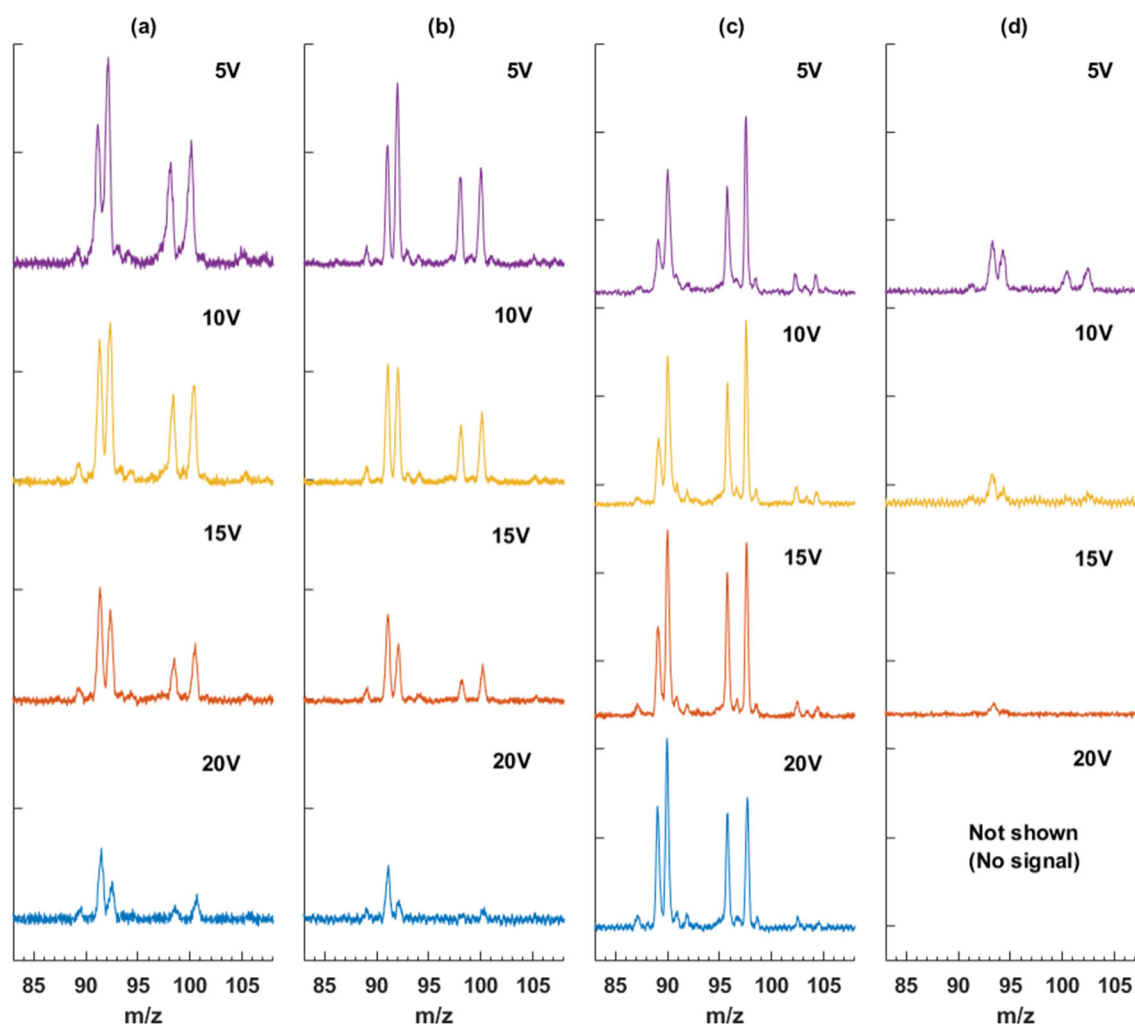


Figure 6. The spectra for toluene mixture with different DC voltages at different displaced positions. (a) -0.24° in pitch. (b) 0.00° in pitch. (c) -0.50 mm in x-displacement. (d) $+0.50$ mm in x-displacement. All the spectra were calibrated based on the spectrum obtained at the assigned “zero” point

will be difficult to predict. On the other hand, the importance and impact of specific DOFs on performance should follow some of the principles observed in the present experiments.

Conclusions

These experiments characterize the sensitivity of a two-plate LIT to electrode misalignment. Among the five degrees of freedom that were studied, pitch has the greatest effect the mass resolution. Z-displacement affects the least on the resolution. The number of ions being detected is affected the most by plate spacing (y -displacement) in the experiments, whereas in the simulation, it is x -displacement that has the largest effect on ion ejection. In any real device, the situation is more complicated, because misalignments in all degrees of freedom occur simultaneously. Nonetheless, understanding the effect of misalignment along a single dimension can guide improvements in design and fabrication of new and smaller devices.

As ion traps are further miniaturized, precise fabrication and alignment of electrodes become an increasing concern and challenge. Although a multi-axis micropositioner was used in these experiments, there is no expectation that such a positioner would be employed in any fieldable device. Rather, electrodes or patterned plates could be aligned using such equipment, and then permanently affixed, prior to including the complete ion trap in a portable instrument. A pre-aligned mass analyzer “cartridge” could be easily replaced in the field, without concern for further alignment or calibration. Additionally, the multi-axis positioner in these experiments provides valuable data on the types and severity of performance degradation to be expected from miniaturized and full-sized ion traps with a non-ideal electrode alignment.

Funding Information

The authors are grateful for the financial support from the National Science Foundation (USA), Chemical Measurement and Imaging Program, award no. 1404886.

References

- Barreira, L.M.F., Parshintsev, J., Karkkainen, N., Hartonen, K., Jussila, M., Kajos, M., Kulmala, M., Riekkola, M.L.: Field measurements of biogenic volatile organic compounds in the atmosphere by dynamic solid-phase microextraction and portable gas chromatography-mass spectrometry. *Atmos. Environ.* **115**, 214–222 (2015)
- Diaz, J.A., Pieri, D., Arkin, C.R., Gore, E., Griffin, T.P., Fladeland, M., Bland, G., Soto, C., Madrigal, Y., Castillo, D., Rojas, E., Achi, S.: Utilization of in situ airborne MS-based instrumentation for the study of gaseous emissions at active volcanoes. *Int. J. Mass Spectrom.* **295**, 105–112 (2010)
- Eckenrode, B.A.: Environmental and forensic applications of field-portable GC-MS: an overview. *J. Am. Soc. Mass Spectrom.* **12**, 683–693 (2001)
- Riedo, A., Bieler, A., Neuland, M., Tulej, M., Wurz, P.: Performance evaluation of a miniature laser ablation time-of-flight mass spectrometer designed for in situ investigations in planetary space research. *J. Mass Spectrom.* **48**, 1–15 (2013)
- Syage, J.A., Hanning-Lee, M.A., Hanold, K.A.: A man-portable, photo-ionization time-of-flight mass spectrometer. *Field Anal. Chem. Technol.* **4**, 204–215 (2000)
- Gao, W., Tan, G., Hong, Y., Li, M., Nian, H., Guo, C., Huang, Z., Fu, Z., Dong, J., Xu, X., Cheng, P., Zhou, Z.: Development of portable single photon ionization time-of-flight mass spectrometer combined with membrane inlet. *Int. J. Mass Spectrom.* **334**, 8–12 (2013)
- Huang, Z., Tan, G., Zhou, Z., Chen, L., Cheng, L., Jin, D., Tan, X., Xie, C., Li, L., Dong, J., Fu, Z., Cheng, P., Gao, W.: Development of a miniature time-of-flight mass/charge spectrometer for ion beam source analyzing. *Int. J. Mass Spectrom.* **379**, 60–64 (2015)
- Getty, S.A., Brinckerhoff, W.B., Cornish, T., Ecelberger, S., Floyd, M.: Compact two-step laser time-of-flight mass spectrometer for in situ analyses of aromatic organics on planetary missions. *Rapid Commun. Mass Spectrom.* **26**, 2786–2790 (2012)
- Li, D., Guo, M., Xiao, Y., Zhao, Y., Wang, L.: Development of a miniature magnetic sector mass spectrometer. *Vacuum.* **85**, 1170–1173 (2011)
- Cheung, K., Velasquez-Garcia, L.F., Akinwande, A.I.: Chip-scale quadrupole mass filters for portable mass spectrometry. *J. Microelectromech. Syst.* **19**, 469–483 (2010)
- Holkeboer, D.H., Karandy, T.L., Currier, F.C., Frees, L.C., Ellefson, R.E.: Miniature quadrupole residual gas analyzer for process monitoring at milli Torr pressures. *J. Vac. Sci. Technol. A.* **16**, 1157–1162 (1998)
- Taylor, S., Tindall, R.F., Syms, R.R.A.: Silicon based quadrupole mass spectrometry using microelectromechanical systems. *J. Vac. Sci. Technol. B.* **19**, 557–562 (2001)
- Schwartz, J.C., Senko, M.W., Syka, J.E.P.: A two-dimensional quadrupole ion trap mass spectrometer. *J. Am. Soc. Mass Spectrom.* **13**, 659–669 (2002)
- Ding, L., Sudakov, M., Kumashiro, S.: A simulation study of the digital ion trap mass spectrometry. *Int. J. Mass Spectrom.* **221**, 117–138 (2002)
- Ouyang, Z., Wu, G., Song, Y., Li, H., Plass, W.R., Cooks, R.G.: Rectilinear ion trap: concepts, calculations, and analytical performance of a new mass analyzer. *Anal. Chem.* **76**, 4595–4605 (2004)
- Badman, E.R., Johnson, R.C., Plass, W.R., Cooks, R.G.: A miniature cylindrical quadrupole ion trap: simulation and experiment. *Anal. Chem.* **70**, 4896–4901 (1998)
- Lammert, S.A., Plass, W.R., Thompson, C.V., Wise, M.B.: Design, optimization and initial performance of a toroidal rf ion trap mass spectrometer. *Int. J. Mass Spectrom.* **212**, 25–40 (2001)
- Badman, E.R., Cooks, R.G.: Special feature: perspective—miniature mass analyzers. *J. Mass Spectrom.* **35**, 659–671 (2000)
- Li, G., Li, D.T., Cheng, Y.J., Pei, X.Q., Zhang, H.Z., Wang, Y.J., Sun, J., Dong, M.: Development of a low power miniature linear ion trap mass spectrometer with extended mass range. *Rev. Sci. Instrum.* **88**, 7 (2017)
- Hendricks, P.I., Dalglish, J.K., Shelley, J.T., Kirleis, M.A., McNicholas, M.T., Li, L.F., Chen, T.C., Chen, C.H., Duncan, J.S., Boudreau, F., Noll, R.J., Denton, J.P., Roach, T.A., Ouyang, Z., Cooks, R.G.: Autonomous in situ analysis and real-time chemical detection using a backpack miniature mass spectrometer: concept, instrumentation development, and performance. *Anal. Chem.* **86**, 2900–2908 (2014)
- Zhai, Y.B., Feng, Y., Wei, Y.Z., Wang, Y.Z., Xu, W.: Development of a miniature mass spectrometer with continuous atmospheric pressure interface. *Analyst.* **140**, 3406–3414 (2015)
- Contreras, J.A., Murray, J.A., Tolley, S.E., Oliphant, J.L., Tolley, H.D., Lammert, S.A., Lee, E.D., Later, D.W., Lee, M.L.: Hand-portable gas chromatograph-toroidal ion trap mass spectrometer (GC-TMS) for detection of hazardous compounds. *J. Am. Soc. Mass Spectrom.* **19**, 1425–1434 (2008)
- Chen, C.H., Chen, T.C., Zhou, X., Kline-Schoder, R., Sorensen, P., Cooks, G.R., Ouyang, Z.: Design of portable mass spectrometers with handheld probes: aspects of the sampling and miniature pumping systems. *J. Am. Soc. Mass Spectrom.* **26**, 240–247 (2015)
- Shortt, B.J., Darrach, M.R., Holland, P.M., Chutjian, A.: Miniaturized system of a gas chromatograph coupled with a Paul ion trap mass spectrometer. *J. Mass Spectrom.* **40**, 36–42 (2005)
- Chaudhary, A., van Amerom, F.H.W., Short, R.T.: Experimental evaluation of micro-ion trap mass spectrometer geometries. *Int. J. Mass Spectrom.* **371**, 17–27 (2014)
- Chaudhary, A., van Amerom, F., Short, R., Bhansali, S.: Fabrication and testing of a miniature cylindrical ion trap mass spectrometer constructed

- from low temperature co-fired ceramics. *Int. J. Mass Spectrom.* **251**, 32–39 (2006)
27. Li, X., Jiang, G., Luo, C., Xu, F., Wang, Y., Ding, L., Ding, C.: Ion trap array mass analyzer: structure and performance. *Anal. Chem.* **81**, 4840–4846 (2009)
 28. Wilpers, G., See, P., Gill, P., Sinclair, A.G.: A monolithic array of three-dimensional ion traps fabricated with conventional semiconductor technology. *Nat. Nanotechnol.* **7**, 572–576 (2012)
 29. Chu, Y., Xiao, Y., Ling, X., Ding, C.: Analytical performance of printed circuit board ion trap array mass analyzer with electrospray ionization. *Fenxi Huaxue.* **41**, 152–158 (2013)
 30. Xu, W., Li, L., Zhou, X., Ouyang, Z.: Ion sponge: a 3-dimensional array of quadrupole ion traps for trapping and mass-selectively processing ions in gas phase. *Anal. Chem.* **86**, 4102–4109 (2014)
 31. Tian, Y., Higgs, J., Li, A., Barney, B., Austin, D.E.: How far can ion trap miniaturization go? Parameter scaling and space-charge limits for very small cylindrical ion traps. *J. Mass Spectrom.* **49**, 233–240 (2014)
 32. Xu, W., Chappell, W.J., Cooks, R.G., Ouyang, Z.: Characterization of electrode surface roughness and its impact on ion trap mass analysis. *J. Mass Spectrom.* **44**, 353–360 (2009)
 33. Ono, T., Sim, D.Y., Esashi, M.: Micro-discharge and electric breakdown in a micro-gap. *J. Micromech. Microeng.* **10**, 445–451 (2000)
 34. March, R.E., Todd, J.F.J. (eds.): Practical aspects of trapped ion mass spectrometry, volume IV: Theory and instrumentation, pp. 373–400. CRC Press, Boca Raton (2010)
 35. Badman, E.R., Cooks, R.G.: A parallel miniature cylindrical ion trap Array. *Anal. Chem.* **72**, 3291–3297 (2000)
 36. Badman, E.R., Cooks, R.G.: Cylindrical ion trap array with mass selection by variation in trap dimensions. *Anal. Chem.* **72**, 5079–5086 (2000)
 37. Misharin, A.S., Laughlin, B.C., Vilkov, A., Takats, Z., Ouyang, Z., Cooks, R.G.: High-throughput mass spectrometer using atmospheric pressure ionization and a cylindrical ion trap array. *Anal. Chem.* **77**, 459–470 (2005)
 38. Tabert, A.M., Greip-Raming, J., Guymon, A.J., Cooks, R.G.: High-throughput miniature cylindrical ion trap array mass spectrometer. *Anal. Chem.* **75**, 5656–5664 (2003)
 39. Wang, L., Xu, F., Ding, C.: Performance and geometry optimization of the ceramic-based rectilinear ion traps. *Rapid Commun. Mass Spectrom.* **26**, 2068–2074 (2012)
 40. Lammert, S.A., Rockwood, A.A., Wang, M., Lee, M.L., Lee, E.D., Tolley, S.E., Oliphant, J.R., Jones, J.L., Waite, R.W.: Miniature toroidal radio frequency ion trap mass analyzer. *J. Am. Soc. Mass Spectrom.* **17**, 916–922 (2006)
 41. Taylor, N., Austin, D.E.: A simplified toroidal ion trap mass analyzer. *Int. J. Mass Spectrom.* **321**, 25–32 (2012)
 42. Ouyang, Z., Badman, E.R., Cooks, R.G.: Characterization of a serial array of miniature cylindrical ion trap mass analyzers. *Rapid Commun. Mass Spectrom.* **13**, 2444–2449 (1999)
 43. Maas, J.D., Hendricks, P.I., Ouyang, Z., Cooks, R.G., Chappell, W.J.: Miniature monolithic rectilinear ion trap arrays by stereolithography on printed circuit board. *J. Microelectromech. Syst.* **19**, 951–960 (2010)
 44. Kothari, S., Song, Q.Y., Xia, Y., Fico, M., Taylor, D., Amy, J.W., Stafford, G., Cooks, R.G.: Multiplexed four-channel rectilinear ion trap mass spectrometer. *Anal. Chem.* **81**, 1570–1579 (2009)
 45. Gear, M., Syms, R.R.A., Wright, S., Holmes, A.S.: Monolithic MEMS quadrupole mass spectrometers by deep silicon etching. *J. Microelectromech. Syst.* **14**, 1156–1166 (2005)
 46. Velasquez-Garcia, L.F., Cheung, K., Akinwande, A.I.: An application of 3-D MEMS packaging: out-of-plane quadrupole mass filters. *J. Microelectromech. Syst.* **17**, 1430–1438 (2008)
 47. Austin, D.E., Wang, M., Tolley, S.E., Maas, J.D., Hawkins, A.R., Rockwood, A.L., Tolley, H.D., Lee, E.D., Lee, M.L.: Halo ion trap mass spectrometer. *Anal. Chem.* **79**, 2927–2932 (2007)
 48. Zhang, Z.P., Peng, Y., Hansen, B.J., Miller, I.W., Wang, M., Lee, M.L., Hawkins, A.R., Austin, D.E.: Paul trap mass analyzer consisting of opposing microfabricated electrode plates. *Anal. Chem.* **81**, 5241–5248 (2009)
 49. Peng, Y., Hansen, B.J., Quist, H., Zhang, Z.P., Wang, M., Hawkins, A.R., Austin, D.E.: Coaxial ion trap mass spectrometer: concentric toroidal and quadrupolar trapping regions. *Anal. Chem.* **83**, 5578–5584 (2011)
 50. Hansen, B.J., Niemi, R.J., Hawkins, A.R., Lammert, S.A., Austin, D.E.: A lithographically patterned discrete planar electrode linear ion trap mass spectrometer. *J. Microelectromech. Syst.* **22**, 876–883 (2013)
 51. Li, A., Hansen, B.J., Powell, A.T., Hawkins, A.R., Austin, D.E.: Miniaturization of a planar-electrode linear ion trap mass spectrometer. *Rapid Commun. Mass Spectrom.* **28**, 1338–1344 (2014)
 52. Wang, Y., Zhang, X., Feng, Y., Shao, R., Xiong, X., Fang, X., Deng, Y., Xu, W.: Characterization of geometry deviation effects on ion trap mass analysis: a comparison study. *Int. J. Mass Spectrom.* **370**, 125–131 (2014)
 53. Tian, Y., Decker, T.K., McClellan, J.S., Bennett, L., Li, A., De la Cruz, A., Andrews, D., Lammert, S.A., Hawkins, A.R., Austin, D.E.: Improved miniaturized linear ion trap mass spectrometer using lithographically patterned plates and tapered ejection slit. *J. Am. Soc. Mass Spectrom.* **29**, 213–222 (2018)
 54. Moxom, J., Reilly, P.T.A., Whitten, W.B., Ramsey, J.M.: Sample pressure effects in a micro ion trap mass spectrometer. *Rapid Commun. Mass Spectrom.* **18**, 721–723 (2004)
 55. Wu, Q., Tian, Y., Li, A., Austin, D.E.: Simulations of electrode misalignment effects in two-plate linear ion traps. *Int. J. Mass Spectrom.* **393**, 52–57 (2015)